

Research Paper

Inhibition of Transient Receptor Potential Vanilloid 6 channel, elevated in human ovarian cancers, reduces tumour growth in a xenograft model

Hui Xue¹, Yuzhuo Wang¹, Tyson J. MacCormack², Tyler Lutes^{2,3}, Christopher Rice³, Michelle Davey³, Dominique Dugourd³, T. Toney Ilenchuk³, and John M. Stewart^{3,✉}

1. Department of Experimental Therapeutics, BC Cancer Agency, 675 West 10th Avenue, Vancouver BC, Canada, V5Z 1L3
2. Department of Chemistry and Biochemistry, Mount Allison University, Sackville, New Brunswick, Canada. E4L 1E4
3. Soricimed Biopharma Inc. 18 Botsford Street, Suite 201, Moncton, NB, Canada, E1C 4W7.

✉ Corresponding author: jstewart@soricimed.com. Soricimed Biopharma Inc. 18 Botsford Street, Suite 201, Moncton, NB, Canada, E1C 4W7. Tel: 1-506-856-0400. Fax: 1-506-856-0414

© Ivyspring International Publisher. This is an open access article distributed under the terms of the Creative Commons Attribution (CC BY-NC) license (<https://creativecommons.org/licenses/by-nc/4.0/>). See <http://ivyspring.com/terms> for full terms and conditions.

Received: 2017.04.18; Accepted: 2017.10.06; Published: 2018.08.06

Abstract

Background: Transient Receptor Potential Vanilloid 6 (TRPV6), a non-voltage gated calcium channel, is implicated in malignancies and correlates with Gleason scores in prostate cancer and with poor prognosis in breast cancer. Data on the TRPV6 status of ovarian malignancies has not received significant attention. The effect of inhibiting TRPV6 activity on ovarian tumour growth has never been reported.

Methods: We quantified TRPV6 mRNA and protein in biopsies of five types of ovarian cancer at different stages and grades by quantitative PCR and immunohistochemistry respectively. We verified the presence of TRPV6 in SKOV-3 cells and xenografts by Western Blotting. NOD/SCID mice bearing xenografted ovarian tumours derived from SKOV-3 were treated daily with TRPV6-antagonistic peptides (SOR-C13 and SOR-C27) at 400, 600 and 800 mg/kg delivered intraperitoneally (i.p.) over 12 days. Data from qPCR and tumour growth experiments were compared with a Student's t-test. Immunohistochemical ranking of staining were compared with Kruskal-Wallis one-way ANOVA and Dunn's Multiple Comparison post-test.

Results: TRPV6 mRNA and protein are significantly elevated at all stages and grades of 5 ovarian cancer types over normal tissue. Overall qPCR log₂ values (n, mean, ± SEM) for mRNA in tumour (n = 165, 5.06 ± 0.16) were greater (p < 0.05) than normal tissues (n = 26, 0.45 ± 0.41). All stages and grades included in the biopsy arrays were significantly greater than normal tissues. Immunohistochemical staining of TRPV6 was ranked >2 (faint in most cells) in 80.5% of tumours (123) while 92% of normal tissues (23) ranked ≤ 2. Daily i.p. injection with SOR-C13 (400, 600 and 800 mg/kg) over 12 days inhibits tumour growth (59%) at the highest dose compared to non-treated controls. SOR-C27 at 800 mg/kg SOR-C27 inhibited tumour growth 55% after 12 days. Results of daily and intermittent dosing (Days 1, 2, 3 and 8, 9, 10) with SOR-C13 were indistinguishable.

Conclusion: TRPV6 mRNA and protein are elevated in biopsies of ovarian cancers compared to normal tissue. Inhibition of TRPV6 activity significantly reduces ovarian tumour growth providing evidence that TRPV6 is a feasible oncology target in ovarian cancers.

Key words: TRPV6, cancer, ovary

Background

Since discovery of Transient Receptor Potential (TRP) ion channels in *Drosophila melanogaster* [1, 2] and subsequent reports of a similar calcium channel in mammals [3, 4] resembling the capsaicin (vanilloid)

receptor [5], membership in this superfamily of 'non-voltage gated' channels expanded to about thirty different channels in six subfamilies in mammals: TRPA (ankyrin), TRPC (canonical), TRPM

(melastatin), TRPML (mucolipin), TRPP (polycystin) and TRPV (vanilloid) [6-9].

A sub-family of TRP channels receiving a great deal of study is the vanilloid group (TRPV) comprised of six members, TRPV1 to TRPV6. The first four channels have close sequence relationship and function sensing heat, acid, stretching/osmotic strain, nociception and pain signal integration (reviewed in [8, 9]). TRPV5 and TRPV6 show lower sequence identity to V1-V4, and different properties. TRPV5 and TRPV6 are selective for calcium ion ($P_{Ca}/P_{Na} \sim 100$) compared to the other four ($P_{Ca}/P_{Na} \sim 1$ to 15), are not ligand-gated and are constitutively active [10]. A major function of these two channels is larger-scale calcium homeostasis. TRPV5 is expressed in distal tubules of the kidneys where it reclaims calcium from pre-urine [11]. TRPV6, while produced in kidney at lower levels than TRPV5, is predominant in the gastro-intestinal tract where it imports calcium, initiating the process by capturing the ion at apical membranes. The protein was reported in placenta, salivary gland, prostate, pancreas, testes, liver and lung [12]. Mice with TRPV6 knock-outs reinforce involvement of this channel in calcium homeostasis [13] showing defective intestinal Ca^{2+} absorption, reduced fertility, and increased urinary calcium.

Over-expression of TRPV6 has been reported in human cancers. TRPV6 mRNA is elevated in a chronic myelogenous leukemia (K-562) and a colorectal cancer cell line (SW480) [14], prostate cancer cell lines LNCaP and PC-3 [12], and leukemia cell lines from rat [15] and human [16]. Immunohistochemistry revealed some TRPV6 in other normal exocrine tissues (e.g. mammary gland, pancreas, prostate) but elevated amounts in carcinomas of exocrine tissues [17, 18]. In advanced prostate cancer [19] where there is a positive correlation of mRNA level with Gleason scores [14], TRPV6-positive prostate tumours show poor prognosis because of a propensity to invade extra-prostatic tissues [20]. Breast cancer biopsies show 2 – 15-fold greater TRPV6 mRNA than healthy tissue [21]. In another study [22] TRPV6 protein was elevated in 93.3% of breast tumour biopsies and elevated TRPV6 in estrogen receptor-negative breast cancers correlated with poor prognosis [23]. While curiously ignored in the wider industrial oncology community, the connection of elevated TRPV6 channels to cancers has been reviewed extensively [24-29].

The role TRPV6 plays in oncology is not clear but calcium-dependent proliferation of cancer cells is influenced by TRPV6 [30]. A reasonable working model for a mechanism of action of elevated TRPV6 is suggested by the collective literature. Sustained elevated cytosolic calcium from increased amounts or

activity of TRPV6 could bind to calmodulin (CaM) that, in turn, activates calcineurin (a CaM/ Ca^{2+} activated phosphatase). Activated calcineurin can activate hyper-phosphorylated Nuclear Factor of Activated T-cells (NFAT) transcription factor [31] which, after translocation to the nucleus [32], activates genes including those influencing cell proliferation and migration. NFAT is a transcription factor for Membrane Type 1 Matrix Metalloproteinase, Matrix Metalloproteinase-type 2 [33] and secreted autotaxin [34, 35]. The latter produces extracellular lysophosphatidyl choline, an activator of Growth Factor Receptor (GFR). The anti-apoptotic nature of increased TRPV6 can be traced to NFAT-dependent, increased production of anti-apoptotic Bcl-2, inhibiting release of mitochondrial cytochrome c and preventing apoptosome formation [36]. Reduction of TRPV6 production in cancer cell lines by silencing-RNA decreases cell proliferation and increases apoptosis, presumably because of NFAT signalling pathway reversion at lower intracellular calcium [21, 37]. Recently, a study of NFAT downstream signalling implicated it in survival and metastasis in breast cancers [38]. In prostate cancer cells (LNCaP, PC-3 and DU-145), increased trafficking of TRPV6 to the plasma membrane under control of Orai1, a protein of the Store-Operated Calcium Channel system, and in association with the Ca^{2+} /S100A11/annexin system, led to increased cell proliferation and reduction of apoptosis. [39]. This report suggested increased TRPV6 activity is a survival response in these prostate cancer cell lines. Reports of work with pancreatic cancers also implicate TRPV6 in calcineurin and NFAT activation where reduced TRPV6 production decreases both [40]. Recently, TRPV6 has been implicated directly in development and prognosis of pancreatic cancer showing decreased survival in patients with elevated tumour TRPV6 levels [41]. Silencing TRPV6 in a number of pancreatic cell lines reduced proliferation and invasion and initiated apoptosis and cell cycle arrest [41].

The inhibitory TRPV6-binding peptides used here (SOR-C13 and SOR-C27) are derived from of the C-terminus of soricidin (accession number P0C2P6), a paralytic peptide from saliva of Northern Short-tailed shrew *Blarina brevicauda*.

SOR-C13 and SOR-C27 bind to and inhibit calcium influx through TRPV6 expressed in HEK-293 cells with EC_{50} values of 14 nM and 65 nM respectively [42]. These peptides delivered a conjugated fluorescent label to TRPV6-rich xenografts of human ovarian cancer (SKOV-3) and prostate cancer (DU-145) and negatively affected a number of epithelial-type cancer cell lines including SKOV-3 in

preliminary *in vivo* and *in vitro* studies [42]. Additionally, a negative contrast MRI agent (Super Paramagnetic Iron Oxide nanoparticles) to which SOR-C27 was chemically attached targeted SKOV-3 xenografts allowing detection and accurate determination of tumour volume [42].

TRPV6 has been viewed as an oncochannel [29] and its gene has been cited as an oncogene [26, 27] or proto-oncogene [39]. Despite this, there are limited data on the status of TRPV6 in ovarian cancer. Only one biopsy sample of an ovarian adenocarcinoma has been reported, and it showed elevated TRPV6 protein [17] compared to minimal staining in normal tissue. We present here the comparative expression of TRPV6 gene in biopsies of all five types [43] of ovarian cancers. Additionally, we report relative levels of TRPV6 protein in biopsies of ovarian tumours as determined by immunohistochemistry. These data support further studies on the functionality of TRPV6 in ovarian cancers and how this dysfunction in intracellular calcium control contributes to cancers. In a recent Phase I clinical trial testing the safety and tolerability of SOR-C13 in various epithelial-type cancers two of four patients with advanced ovarian cancer showed stable disease after two cycles of treatment [44].

A secondary aim was to determine the effect of TRPV6 inhibitors on TRPV6-rich xenografts as part of an assessment of this channel as a therapeutic target. Reported here are the effects of antagonistic, TRPV6-inhibiting peptides in reducing the growth of human ovarian xenografts in NOD/SCID mice. The data met the objectives to assess TRPV6 as a target in ovarian cancer and, having shown that, that inhibiting the TRPV6 oncochannel is a reasonable therapeutic strategy.

Methods

Determination of TRPV6 mRNA levels in biopsies.

TRPV6 mRNA levels in ovarian cancer biopsies were compared to normal ovary tissue. Human TRPV6 and β -actin mRNA levels were determined in 191 ovarian biopsies, in triplicate, using the TissueScan Ovarian Cancer cDNA Array 1, 2, 3 and 4 (cat. nos. TSC10125-HORT101, TSC10126-HORT102, TSC10127-HORT103 and TSC10128-HORT104) from OriGene Technologies, Rockville MD. Pathologies of individual biopsies are given in Supplementary Table S1. The vendor did not divulge primer and probe sequences for TaqMan assays. The TRPV6 gene expression assay used was Hs00367960_m1, and produces a 72 bp amplicon containing base pair 1347 in the middle of RefSeq NM_018646.4, the boundary

between exons 8 and 9. This probe was labeled with FAM (6-fluorescein amidate). The β -actin gene expression assay used was VIC-labeled (2'-chloro-7'-phenyl-1,4,-dichloro-6-carboxy-fluorescein) assay Hs99999903_m1 that produces a 171 bp amplicon containing base pair 53 on the N-terminal end of RefSeq NM_001101.3, the exon 1-2 boundary. There was no cross reactivity with genomic DNA in qPCR.

The cDNAs in each array sample were normalized to β -actin as recommended by the supplier. TRPV6 gene expression was determined using qPCR and TaqMan[®] probes for TRPV6 (Target) and β -actin (reference gene) from Life Technologies[™] in duplex reactions. A master mix was prepared as 1 X PerfeCTa[®] FastMix[®] II (Quanta BioSciences[™] Gaithersburg MA, USA), 1 X TRPV6 primer/probe, 0.5 X β -actin primer/probe and RT-PCR grade H₂O (Ambion catalogue no. AM9935). qPCR was carried out at 95°C for 10 s followed by 60°C for 30 s for 40 cycles. The levels of TRPV6 gene expression in tumour biopsies (Target) were normalized to β -actin (reference gene) and assessed relative to the mean of all normal biopsies (Calibrator) that were also normalized to β -actin. The relative expression levels (R) were calculated using the $\Delta\Delta C_T$ method. We found the variability in C_T values for the reference gene (β -actin) acceptable for the purposes of this study. Comparison of the mean C_T values (\pm SEM) for β -actin in normal tissues (24.47 ± 0.19 ; $n = 27$) and cancerous biopsies (25.05 ± 0.11 ; $n = 165$) revealed no statistical difference (Mann Whitney). Additionally, the medians of the two groups were not significantly different. The stark differences between the mean $2^{(-\Delta\Delta C_T)}$ values of normal tissue (3.03 ± 0.71) and cancerous tissue (90.05 ± 16.3) greatly overshadow any variation in the housekeeping gene expression.

Immunohistochemical assessment of TRPV6 protein in ovarian biopsies

TRPV6 immunohistochemical staining was carried out with normal (23) and ovarian cancers (123) biopsies from commercial sources. Tissue microarrays (TMAs) were obtained as formalin-fixed, paraffin-embedded (FFPE) cores (US BioMax Inc., Rockville, MD 20850, USA; catalogue Numbers OV483, OV802, BCN721 and T112). Pathology descriptions of biopsies are provided in Supplementary Table S2. FFPE slides were deparaffinized, rehydrated and processed by microwave heat-induced epitope retrieval in 10 mM sodium citrate/0.05% Tween 20 buffer, pH 6.0 (US Biomax protocols). Rabbit anti-TRPV6 antibody (Millipore, Catalogue No. AB9336, 10 μ g/mL) was used and bound anti-TRPV6 antibody was detected

with a goat anti-rabbit secondary antibody (Santa Cruz, Cat. No. sc-2030, antibody ID AB 631747) using the Lab Vision™ UltraVision™ ONE Detection System: HRP/DAB Plus Chromagen (ThermoFisher Scientific). Slides were counterstained in Mayer's Hematoxylin solution for 60 seconds. TMAs were imaged with a Nikon Eclipse Ti-E Inverted microscope with Nikon CF160 objectives and color CCD camera (1024 x 768). The antigen used to generate the rabbit TRPV6 polyclonal antibody was a synthetic peptide corresponding to amino acids 752 to 765 of human TRPV6 (accession number Q9H1D0.3; sequence NRGLEDGESWEYQI). PBLAST on *H. sapiens* shows only a TRPV6 match with the closest next match was on RGLD sequence to DGCR14 isoform X5 (78% identity and an E value of 6.8 on the total query) suggesting little sequence identity outside TRPV6 including all other TRPV channels. Tissue array slides having normal and cancerous ovarian cores were used to optimize conditions for IHC and to test controls for antibody specificity. As a negative control, tissues were incubated without primary antibody (diluent only). No staining was observed in negative controls. As a positive control for specificity, the TRPV6 antibody was pre-incubated with a 10-fold excess of peptide corresponding to the antigen amino acid sequence prior to development of ovarian tissue cores. Significantly reduced staining of tissues was observed with neutralized antibody. Further validation of the primary antibody was obtained by staining, as a positive control, the apical domain of renal tubular cells known to contain TRPV6: appropriate staining patterns for the TRPV6 population was observed. A guide to the intensity ranking of TRPV6-staining (0 to 5) is shown in Supplementary Figure S1: Ranking: 0 = no tissue staining; 1 = majority of cells negative with weak staining in some cells; 2 = weak staining of a majority of cells; 3 = light staining of a majority of cells; 4 = moderate staining of a majority of cells; 5 = intense staining of a majority of cells.

SKOV-3 Cell Culture and Xenografts

Validated SKOV-3 cells (ATCC #HTB-77) were obtained from the American Type Cell Collection (ATCC) and grown under conditions specified by the ATCC at 37°C and 5% CO₂ in McCoy's 5a medium containing fetal bovine serum (10% v/v). SKOV-3, an ovarian adenocarcinoma isolated from ascites, shows resistance to a number of cytotoxic agents. SKOV-3 shows amplified HER-2 and mutated *PIK3CA* (phosphatidylinositol-4, 5-bisphosphate 3-kinase catalytic subunit α) and *ARID1A* (AT-rich Interactive Domain-containing protein 1A) [45] involved in chromatin modification and tumour suppression [46].

SKOV-3 produces xenografts described to be like clear cell adenocarcinoma [47]. The presence of TRPV6 protein in SKOV-3 tumours was confirmed in excised tumours (see results).

SKOV-3 cells (1.5×10^6 cells/graft) were injected subcutaneously at 4 sites on the backs of six female NOD/SCID mice to establish the xenografts. Tumour growth was monitored daily and two weeks after implantation solid tumours became visible. Four to six weeks after SKOV-3 cell injection, tumour sizes were large enough and mice were grouped randomly into experimental groups. This arrangement allowed for the production of a larger number of tumours for this proof of concept study.

Western Blots for TRPV6 in tumour lysates

Lysate supernatants for Western Blot testing were prepared by homogenizing excised cells or control tumours in RIPA lysis buffer (Santa Cruz, Cat# sc-24948) containing Protease Inhibitor cocktail and PMSF (phenyl methyl sulfonyl fluoride), and centrifuging at 10,000xg. NuPage 4-12% Bis-Tris Gels (1.5 mm x 10 well; ThermoFisher Scientific, Cat. No. NP0335BOX) with NuPage MOPS SDS Running Buffer 20X (ThermoFisher, Scientific Cat. No. NP0001) were used for SDS PAGE electrophoresis. Protein (50 μ g) was loaded in each well. Developed gels were electroblotted onto PVDF membranes (Bio-Rad, Immuno-Blot PVDF Membrane, 0.2 μ m; Cat. No. 162-0177) using the iBlot® system and antibody incubations were performed using the SNAP i.d. system from Millipore. ECL Advance™ western blotting detection kit (Fisher Cat #45001173) was used to detect the protein expression. The primary rabbit anti-TRPV6 antibody (towards amino acids 704 - 725 of the TRPV6 C-terminus) was developed for in-house use by AgriSera AB (Vännäs, Sweden). This antibody was validated against a commercial rabbit anti-TRPV6 antibody (Santa Cruz, H-90, Cat. No. sc-28763, antibody ID AB 2209543, 1/200 dilution) developed against amino acid residues 636 - 725 of the C-terminal of TRPV6. Both antibodies were tested against lysates of TRPV6-producing prostate cancer cell line PC-3. The secondary antibody, a goat anti-rabbit IgG-HRP (horseradish peroxidase) (Santa Cruz, Cat. No. sc-2030, antibody ID AB 631747, 1/5000 dilution), was used to develop the blot after blocking with non-fat milk powder. ECL Advance™ western blotting detection kit (Fisher Cat. No. 45001173) was used to detect the HRP-tagged secondary antibody. Images of the gels were captured with an Alpha Innotech imager (Filter #3, aperture #2.8) and a 10 min exposure time. In a separate experiment the synthetic antigen was incubated with the in-house primary antibody overnight to neutralize

it and used to execute blots to confirm the banding observed was due to TRPV6.

Animals

Female NOD/SCID mice (6 – 8 week old, 20 – 25 g) were purchased from JAX[®] Mice, Clinical & Research Services (Jackson Laboratory, Bar Harbor, Maine 04609 USA) and housed in Animal Research Centre of the British Columbia Cancer Research Centre in pathogen-free conditions. All food, water and bedding were sterilized prior to use. Temperature (20–21°C) and humidity (50–60%) were controlled with daily cycles of 12 h light and 12 h dark. Cages were changed twice a week. All experiments were carried out in accordance with the guidelines of the Canadian Council on Animal Care and approved by the Animal Care Committee of the University of British Columbia (Application #A10-0082). All efforts were made to minimize animal discomfort. All animals were assessed for health prior this study and were monitored for change in body mass, diarrhea, heavy panting and ruffling of fur as symptoms of distress.

Peptide synthesis and characterization

An acetate salt of SOR-C13 (KEFLHPSKVLDLPR) was synthesized by solid-phase methods (Bachem Americas Inc., Torrance, California, USA) and used in dose response and dose scheduling experiments. This product had a molecular mass of 1565.9 Da, a peptide purity of 99.3% with a peptide content of 83.7% providing a correction factor from bulk-to-need peptide of 0.831. Endotoxin level (LAL test) was <0.02 International Units and thus acceptable for this preparation. SOR-C27 (EGKLSSNDTEGGLCKEFLHP SKVDLPR) was synthesized as a trifluoroacetate salt (CanPeptide, Montreal, Canada) from quality assured starting materials without endotoxins. This product showed a molecular mass of 2957 Da, a peptide purity of 95% with a peptide content of 65% providing a correction factor of bulk-to-need peptide of 0.618. All peptide doses are reported here in terms of bulk peptide preparations (mg/kg).

Drug preparation and administration

Peptides were dissolved and diluted with sterile saline daily to prepare 40 mg/mL, 60 mg/mL and 80 mg/mL stock solutions. Dissolved peptides were administered by intraperitoneal (i.p.) injection at 0.1 mL/10 g body weight daily or intermittently as summarized below. Carboplatin solution (10 mg/mL) was diluted with sterile saline to 6 mg/mL. Paclitaxel (6 mg/mL) stock solution was freshly diluted with sterile saline to 1.8 mg/mL. Chemotherapeutic drug doses were administered by i.p. injection at 0.1 mL/10 g body weight with

Paclitaxel injected first, followed by carboplatin 30 min later. For dose response experiments animals were injected i.p. daily on Days 1 to 12 with 400 mg/kg, 600 mg/kg or 800 mg/kg of SOR-C13 or SOR-C27. A dose scheduling experiment compared daily dosing with SOR-C13 to dosing on Days 1-3 and Days 8-10 at the same doses. The negative control was saline (injected the same day as peptide treatment) and the positive control was a combination of carboplatin (60 mg/kg) plus Paclitaxel (18 mg/kg) injected i.p. on Day 1 and Day 8.

Data analysis

Tumour volumes were estimated ($L \times W \times H \times 0.52$) from caliper measurements. The percentage growth inhibition stated is %T/C and calculated as $100 - (\Delta T \times 100 / \Delta C)$, where ΔT and ΔC are changes in treated and control tumour volumes respectively, over the treatment period. Statistical comparison of the treatment groups and study days was done with the Student's t-test. Analysis of the qPCR data was by comparison of mean log₂ values with the Student's t-test. All data cited in this report are mean \pm SEM. Statistical comparisons of the intensities of IHC staining were made using Kruskal-Wallis one-way ANOVA and Dunn's Multiple Comparison post-test. Statistical significance was taken as $p \leq 0.05$ in all comparisons. Statistical analysis and graphics were generated with Prism 5 from GraphPad.

Results

The TRPV6 gene becomes abnormally active in ovarian cancer

While it is not clear when TRPV6 gene becomes so active in the trajectory leading to ovarian cancer, its mRNA and protein are clearly elevated at early cancer stages, and in all five types of ovarian cancer. Relative TRPV6 mRNA levels in normal tissue biopsies were compared to tumour biopsies of various stages, grades and subtypes (Figure 1A – E). The mean \pm SEM log₂ value of all cancer biopsies ($n = 165$; 5.06 ± 0.16) was significantly greater ($p < 0.05$) than normal tissues ($n = 26$; 0.45 ± 0.41) (Figure 1A). Mean log₂ values of all tumour biopsies to normal tissues showed a significant difference in means of about 5 units (about 34-fold) and a maximum difference of about 11 log₂ units (about 2000-fold).

When examined in reference to cancer stage, there were no statistical differences between the mean log₂ values of Stage I, II, III or IV so they were grouped as Early (Stage I+II) and Late Stages (III+IV) (Figure 1B). Both Early ($n = 49$; 4.58 ± 0.32) and Late Stage samples ($n = 78$; 5.47 ± 0.21) contained more TRPV6 mRNA than normal tissues ($p < 0.05$). Late

Stage tumours showed greater *TRPV6* expression than Early Stage ($p < 0.05$). There were no statistical differences in mean *TRPV6* mRNA amounts between degrees of differentiation (Grade) of tumour cells (Figure 1C). Well-differentiated (G1: $n = 12, 4.83 \pm 0.88$), moderately differentiated (G2: $n = 45, 5.61 \pm 0.25$) and poorly differentiated (G3: $n = 82, 5.08 \pm 0.23$) tumours all showed about 5 more log₂ units (32-fold) *TRPV6* mRNA than normal tissue ($p < 0.05$). We compared five histological sub-types of ovarian

cancer and observed that all subtypes expressed significantly more ($p < 0.05$) *TRPV6* mRNA than did normal tissue (Figure 1D). Clear cell ($n = 10, 4.27 \pm 0.91$), endometrioid ($n = 28, 4.82 \pm 0.44$), high-grade serous ($n = 82, 5.50 \pm 0.18$) and mucinous adenocarcinomas had more *TRPV6* mRNA ($n = 5, 3.25 \pm 0.99$) than normal tissues ($p < 0.05$). Low-grade serous adenocarcinoma was not statistically evaluable ($n = 2$) but showed a mean log₂ relative expression of 5.37.

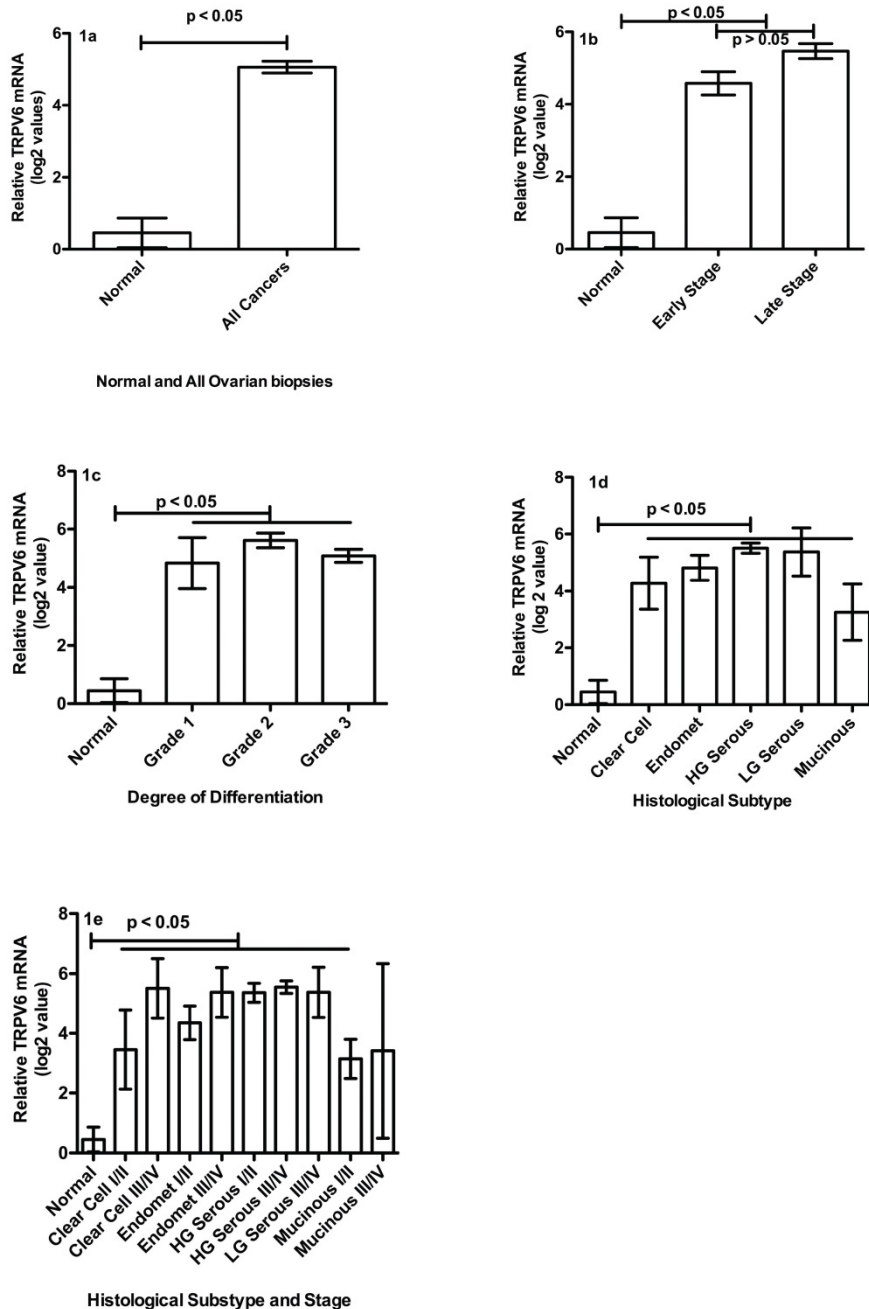


Figure 1: *TRPV6* mRNA levels in ovarian cancer biopsies compared to normal ovary tissue. **(1A)** Comparison of normal ($n = 26$) and all cancer biopsies ($n = 165$): the mean \pm SEM log₂ value of all biopsies. **(1B)** Comparison of *TRPV6* mRNA log₂ values for normal ($n = 26$) and Stages of tumour biopsies. Early Stage $n = 49$; Late Stage $n = 78$. **(1C)** Comparison of log₂ values for normal and Grades of tumour biopsies. Grade 1 $n = 12$; Grade 2 $n = 45$; Grade 3 $n = 82$. **(1D)** Comparison of *TRPV6* mRNA log₂ values based on histological subtype (for all stages). Endomet = Endometrioid; HG = High Grade; LG = Low Grade; Mucinous $n = 5$; Clear Cell $n = 10$; Endomet $n = 28$; HG serous $n = 82$; LG Serous $n = 2$. **(1E)** Comparison of *TRPV6* mRNA log₂ values for various cancer subtypes at Early (I/II) and Late Stages (III/IV); Mucinous (I/II) $n = 3$; Mucinous (III/IV) $n = 2$; Clear Cell (I/II) $n = 6$; Clear Cell (III/IV) $n = 4$; Endomet (I/II) $n = 20$; Endomet (III/IV) $n = 8$; HG Serous (I/II) $n = 20$; HG Serous (III/IV) $n = 62$; LG Serous (III/IV) $n = 2$. Abbreviations: HG = High Grade; LG = Low Grade; Endomet = Endometrioid. Plotted values represent the mean \pm SEM for various categories.

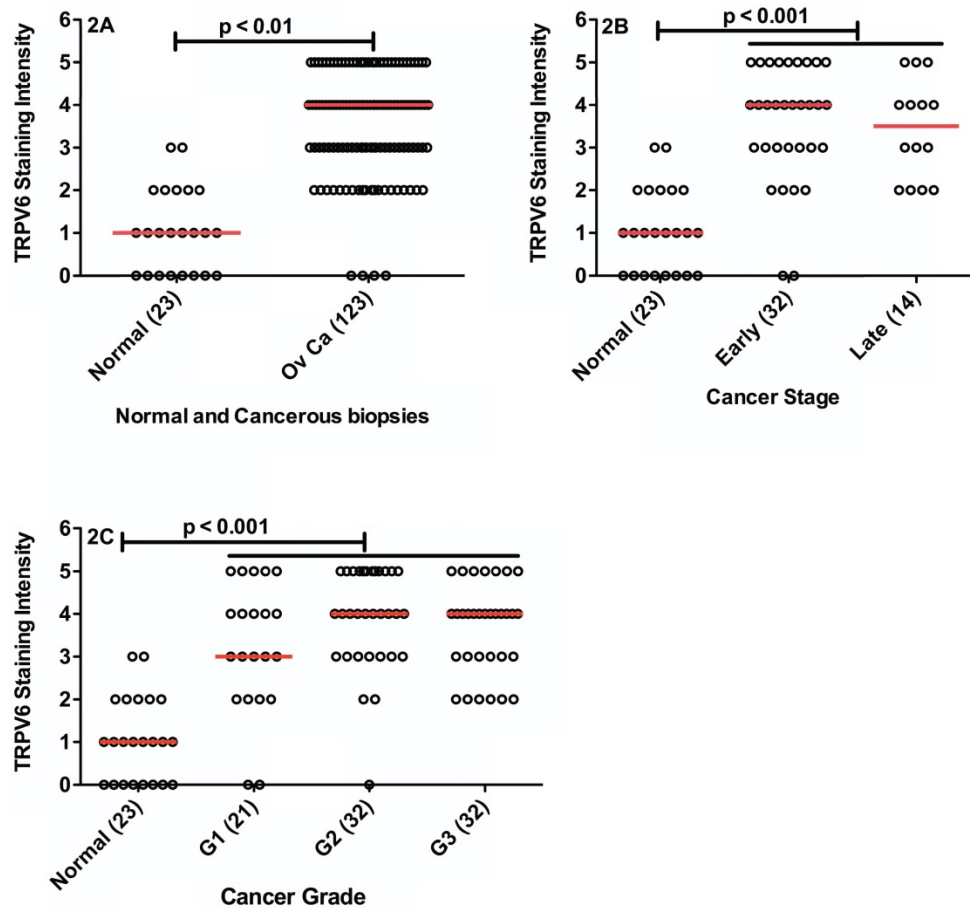


Figure 2: TRPV6 immunohistochemical staining in normal (23) and various ovarian cancer types (123). Each biopsy is represented by a data point, with the horizontal, red bar representing the median value in the category. **(2A)** Comparison of TRPV6 staining in normal tissue biopsies and all neoplasms (Ov Ca = ovarian cancer). **(2B)** Comparison of TRPV6 staining in normal tissue, and Early (I+II) and Late (III+IV) Stage tumours. **(2C)** Comparison of TRPV6 staining in normal tissues and tumour grade (G1 = Grade 1; G2 = Grade 2; G3 = Grade 3). The values in parentheses are the numbers of biopsies tested.

A detailed examination of data, separating Early and Late Stages of the ovarian cancer subtypes (Figure 1E), indicated a number of subtypes/stages had significant greater log₂ values than normal tissue: Clear cell Early Stage (n = 6, 3.45 ± 1.32 , $p < 0.05$), clear cell Late Stage (n = 4, 5.50 ± 1.00 , $p < 0.05$), endometrioid Early Stage (n = 20, 4.35 ± 0.56 , $p < 0.05$), endometrioid Late Stage (n = 8, 5.37 ± 0.84 , $p < 0.05$), high-grade serous Early Stage (n = 20, 5.36 ± 0.32 , $p < 0.05$), and High-grade serous Late Stage (n = 62, 5.55 ± 0.21 , $p < 0.05$) contained more TRPV6 mRNA than normal tissue biopsies. While Mucinous Early Stage (n = 3, 3.15 ± 0.65 , $p < 0.05$) was significantly richer in mRNA than normal tissue, Mucinous Late Stage (n = 2, median = 3.49) was not statistically comparable because of the low sample number. There were no samples representing Low Grade Early Stage adenocarcinomas and only 2 Late Stage samples in this panel (mean = 5.27 ± 0.84).

Increased TRPV6 appears to translate into elevated levels of TRPV6 protein produced by SKOV-3 xenografts. The intensity of IHC staining of all tumour biopsies compared to normal tissue

biopsies is shown in Figure 2A. Normal tissue biopsies showed significantly less staining than the combined ovarian cancer biopsies ($p < 0.05$). Only 4 (3.3%) of tumour biopsies showed no staining for TRPV6 and all others were greater than a score of 2. Normal tissues showed none or very weak staining (ranked 0 – 1) in 70% of the samples with 22% at rank 2, and 8.7% above a 2 ranking. There was a statistically significant difference between the median intensity values indicating TRPV6 protein expression is elevated in the cancer samples.

For those biopsies with available staging data we assessed Early (Stage I and II) and Late (Stage III and IV) samples (Figure 2B) and observed that TRPV6 protein expression was similar in both categories. Early (I + II) and Late Stage (III + IV) cancers both showed greater TRPV6 staining in comparison to normal tissue ($p < 0.05$) but no difference between the staging categories. There were no differences in TRPV6 staining between well, moderately and poorly differentiated tissues (Figure 2C) but all staining intensities were significantly greater than normal samples ($p < 0.05$).

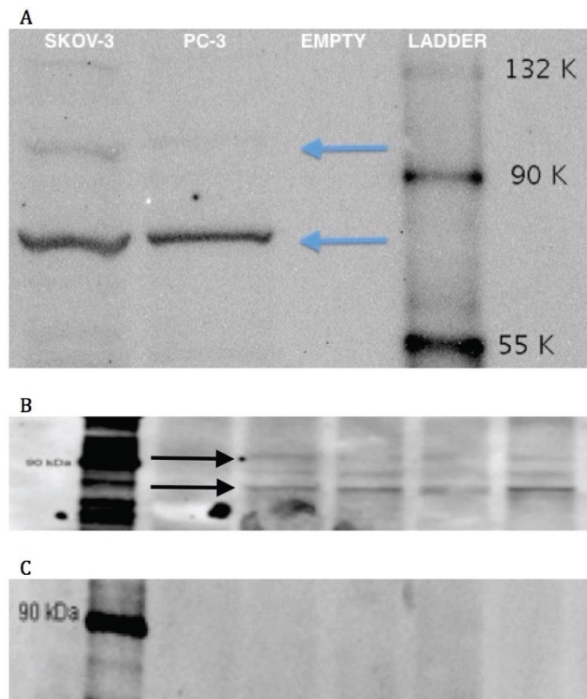


Figure 3: Western Blots of SKOV-3 cells and tumours growth with them. **3A:** Western blot of a lysate of cultured SKOV-3 cells including a known TRPV6-containing PC-3 lysate; 'empty' indicates a lane with only sample buffer and no lysate added. **3B:** Western blot of four lysates of control SKOV-3 xenograft tumours (no treatment). **3C:** Antibody neutralization: peptide antigen incubation of primary antibody before contact with electrophoretic gels from lysates of SKOV-3 xenograft tumours.

TRPV6-inhibiting peptides reduce growth of TRPV6 producing ovarian xenografts in mice.

Production of TRPV6 protein is shown in a Western Blot of cultured SKOV-3 cells (Figure 3A) while its presence in xenografted control tumours of SKOV-3 is shown in Figure 3B. In both instances bands for fully glycosylated (93 kD) and fully deglycosylated protein (85 kD) are shown along with an intermediate species. A separate antibody neutralization experiment wherein the primary antibody was pre-incubated with the synthetic peptide antigen showed an absence of these bands (Figure 3C) confirming the presence of this epitope sequence in those bands.

The dose response and time course for SKOV-3 xenografts for two dosing regimens of SOR-C13 are shown in Figure 4A and 4B. Results from a daily dosing regimen for 12 days are very similar to results from a dosing regimen with treatment on days 1, 2, 3, 8, 9 and 10. While there appears to be some small dose response in daily dosing early in the time-course, both regimes saturate the effect at the lowest dose (400 mg/kg). By Day 12 of daily dosing all treatments produced statistically significant reduction in tumour growth. There was no significant difference in growth between the doses at Day 12 of daily peptide dosing. While SOR-C13 doses of 400 mg/kg ($p = 0.001$) and

600 mg/kg ($p = 0.002$) showed significantly less tumour suppression than CAT treatment with 800 mg/kg, peptide was not different than the CAT treatment ($p = 0.098$).

Intermittent SOR-C13 dosing showed similar results as daily dosing. All treatments resulted in suppressed tumour growth compared to the control and all treatments were significantly less than the response to CAT. Comparisons of each SOR-C13 dosing schedule (daily versus intermittent) showed no significant difference between the mean reductions of tumour volume.

The dose response experiment using SOR-C27 is shown in Figure 5. There was a suggestion of a dose response in tumour growth suppression but the trend was not statistically significant. After 12 consecutive days of dosing with SOR-C27 growth rates were suppressed 42.8%, 49.0% and 55.5% (%T/C values) for 400 mg/kg, 600 mg/kg and 800 mg/kg respectively, while CAT decreased tumour growth 44%. Finally, the authors note that scrambled peptides may have been better controls than injection vehicle but their use in an *in vivo* system would also raise issues of changes in stability and pharmacokinetic profiles that may confound interpretation of effects.

Mouse health was monitored during the experiments for signs of stress, including loss of body weight, diarrhea, heavy panting and ruffling of fur. Mice dosed daily with SOR-C13 had about 5% weight loss, the intermittent schedule produced no weight loss and the CAT produced an 8% weight loss. Mice receiving SOR-C27 lost 5.8%, 9.5%, and 13.7% at 400 mg/kg, 600 mg/kg and 800 mg/kg with CAT treatment showing a 9.7% loss in body mass. All mice in the two SOR-C13 dose groups (daily and intermittent), as well as the control group, had normal fur while mice receiving chemotherapeutic drugs showed some ruffling of fur, but were within health standards requirements. All animals were considered healthy on the basis of behaviour, activity and food consumption. Gross organ examination at the end point showed that a daily dose of 400 mg/kg and 600 mg/kg of SOR-C27 was not toxic. However, there was some liver swelling in the group treated with SOR-C27 at 800 mg/kg (100% incidence).

Discussion

The TRPV6 gene is highly active in ovarian cancers of all subtypes, stages and grades compared to healthy tissue. This result is consistent with reports on prostate and breast cancers. Both Early Stage, when the lesion is largely contained in the ovary and nearby pelvic organs (e.g. fallopian tubes, uterus, etc.) and Late Stage, when there are metastases to other abdominal organs (e.g. peritoneum, lymph nodes)

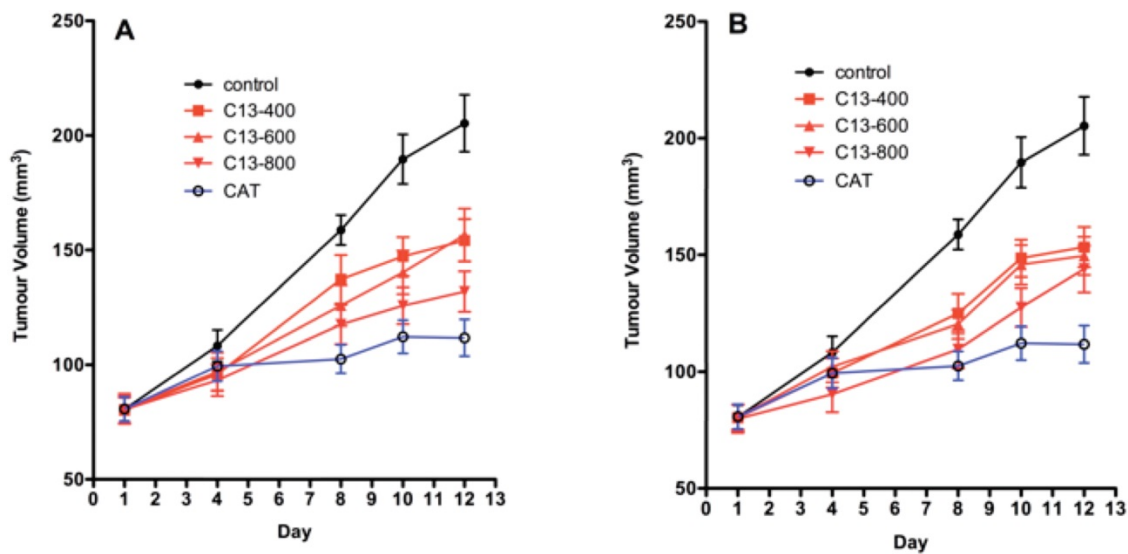


Figure 4: Tumour volumes in the SKOV-3 xenograft model in mice. **A)** Daily SOR-C13 dosing (days 1 to 12) of SKOV-3 xenografts at 400, 600 and 800 mg/kg; **B)** Intermittent SOR-C13 dosing at 400, 600 and 800 mg/kg on days 1, 2, 3, 8, 9 and 10. CAT = carboplatin and taxane (paclitaxel) dosing days 1 and 8. Data are mean \pm SEM, n = 24 and 20 (for CAT treatment) representing 6 and 5 mice. Note: This work was done as a single experiment and the growth curves for 'no treatment' and for CAT treatments are the same.

and extension to distant sites (liver, lung, brain etc.) showed significantly greater TRPV6 gene expression than normal tissue. As a measure of the comparative levels we calculated the sensitivity and selectivity of median log₂ values of TRPV6 mRNA using an arbitrary cut-off value of 1 (a 2-fold excess of mRNA) as would typically be done for diagnostic tests. The sensitivity value indicated a 96.4% probability of greater than 2-fold excess of TRPV6 mRNA when the disease was present. The specificity value indicated a 73.1% probability of there being less than 2-fold more mRNA when the disease was absent. This discrimination extends to the five disease subtypes under the ovarian cancer umbrella, where all showed greater signal than healthy tissue. No significant differences between Early and Late Stage conditions of the individual five subtypes were observed. While all Grades of ovarian tumour were significantly greater than normal tissue, there was no statistical distinction between levels of differentiation. This was different than reported in breast and thyroid cancers [17] where well-differentiated samples expressed lower levels of TRPV6. Thus, elevation of TRPV6 mRNA seems an event that occurs by Early Stage in all types of ovarian cancer with the possible exception of Low Grade serous adenocarcinoma where there were no samples. These data indicate that TRPV6 mRNA levels may provide a promising biomarker for the presence of ovarian cancer in general although not one that would be predictive of stage or grade. Subtler differences, particularly between the various ovarian cancer types, may become apparent if a more sensitive housekeeping gene than β -actin was used. The abundance of β -actin mRNA tends to mask smaller differences between samples.

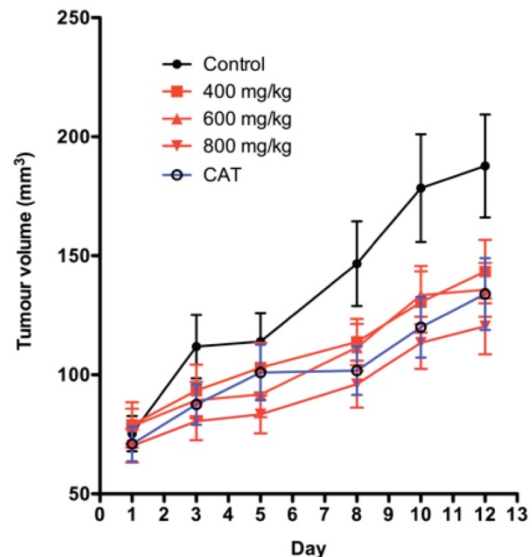


Figure 5: The effect of SOR-C27 on SKOV-3 xenograft tumour volume in mice. The doses of SOR-C27 were 400, 600 and 800 mg/kg. CAT = Carboplatin plus Taxane (paclitaxel). The data are mean \pm SEM, n = 24 (20 for control) tumours in 6 (5 for control) mice. Note that preliminary data for 400 mg/kg was previously presented in Bowen et al. 2013 [42].

Since TRPV6 has been linked to proliferation and progression of some cancers it was necessary to assess whether elevated TRPV6 mRNA translates to increases in TRPV6 protein in ovarian cancer cells. The IHC assessment of the amount of ion channel across all types, stages and grades of ovarian cancer biopsies indicated TRPV6 protein levels, like TRPV6 mRNA expression, were elevated. Using the same approach as above to compare cancer versus normal we assessed the diagnostic utility of TRPV6 protein staining using IHC. Using a cut-off ranking of 2 (mild TRPV6 staining in most cells) we can estimate the sensitivity of this IHC assessment as 80.5% and the

specificity as 91.3%. Thus, about 80% of the tumours showed staining greater than a rank of 2, while 90% of normal tissue was below or at this staining intensity. Since TRPV6 has been implicated in increased cell proliferation, similar TRPV6 protein expression levels in slow growth (Grade I) and rapid growth (Grade III) tumours implies another level of regulatory complexity. Late stage tumours showed greater gene activity than Early Stage (Fig 1B) but similar levels of TRPV6 protein (Fig 2B) suggesting that a closer examination of translational, post-translational and regulatory control of the TRPV6 system in ovarian cancer may provide interesting insights. Another layer of complexity could be the degree of deglycosylation of the channel. Mature TRPV6 is N-glycosylated [48] but exists in two major forms: a fully glycosylated ion channel and one with modified or absent oligosaccharide. Klotho, a beta-glucuronidase linked to aging, is thought to play a part in initiating deglycosylation of TRPV6 [49] and is up-regulated in ovarian cancer [50]. Removal of sialic acid residues capping the oligosaccharide attached to TRPV6 increases its membrane residence time [51] while deglycosylated TRPV6 has increased calcium flux activity [49, 52]. A more extensive validation of anti-TRPV6 antibodies will be required in future studies but there were large differences between staining intensity of normal and cancerous ovarian biopsies with the antibody used here.

Data herein represent the only comprehensive study of TRPV6 expression in ovarian cancer. There is only one report in the literature of elevated TRPV6 protein in a single ovarian adenocarcinoma [17] and thus these data suggest a closer examination was overdue. There were not enough 5-year survival data to provide a meaningful assessment of any correlation with TRPV6 mRNA levels at this stage of the work (42 out of the sample set). When TRPV6 was inhibited, decreased *in vitro* cell viability resulted [42]. It is likely that TRPV6 plays a role in transformed ovary cells that is similar to that reported for both prostate and breast cancers.

In SKOV-3 tumours all dose levels of SOR-C13 resulted in reduction of tumour growth but only a small indication of a dose response. There were insignificant differences in response to SOR-C13 dose schedules tested (daily versus intermittent). The similarity in response at all peptide dosing levels and dosing schedules may result from saturation of TRPV6 'peptide receptors' at concentrations of peptides used. Part of the saturation effect may reflect a dwell time at the tumour since a SOR-C13 tagged with fluorescent Cy5.5 remains at the tumour site for at least 3 days [42]. Inhibition of TRPV6 by the two peptides resulted in tumour growth suppression

similar to the responses to CAT. Note that, after correcting for concentration differences (bulk peptide to neat peptide and mole equivalents), SOR-C27 appears to be about 2.5-fold more active than SOR-C13 on a molar basis: 665 mg/kg of neat SOR-C13 (425 μ mole/kg) provides 59% inhibition of tumour growth while 494 mg/kg of neat SOR-C27 (167 μ mole/kg) produces similar inhibition (55%).

Conclusions

Inhibition of TRPV6 calcium flux by SOR-C13 or SOR-C27, with subsequent reduction in tumour growth rate, supports TRPV6 as an oncology target and supports the further development of soricidin-derived peptides treat epithelial-derived cancers, including ovarian cancer. TRPV6 is overexpressed throughout progression of various histological manifestations of ovarian cancer. An exception could be Early Stage Low Grade serous adenocarcinoma that wasn't included in the sample set. A mechanism for TRPV6 involvement in the progression and proliferation of ovarian cancer is still unclear. Whether NFAT/calcineurin pathways and downstream anti-apoptotic events are active in ovarian cancers, as reported for prostate cancers [37], is not known, but is a reasonable starting point for further study. In light of proliferative and anti-apoptotic roles this ion channel plays, the data from pre-clinical and clinical studies support the potential therapeutic utility of targeting TRPV6 ion channels.

Abbreviations

TRPV6: Transient Receptor Potential Vanilloid six; mRNA: messenger Ribonucleic Acid; PCR: polymerase chain reaction; qPCR: quantitative polymerase chain reaction; NOD/SCID: Non-obese Diabetic/Severely combined immune-deficient; ANOVA: Analysis of Variance; P_{Ca}/P_{Na} : ratio of permeation of calcium to sodium; CaM: calmodulin; NFAT: Nuclear Factor of Activated T-cells; GFR: growth factor receptor; Bcl-2: B-cell lymphoma-2; cDNA: cloned Deoxyribonucleic Acid; bp: base pair; FAM: 6-fluorescein amidate; VIC-labeled: 2'-chloro-7'-phenyl-1,4,-dichloro-6-carboxy-fluorescein; TMA: tissue microarray; FFPE: formalin-fixed, paraffin-embedded; IHC: immunohistochemistry; ATCC: American Type Cell Collection; HER-2: human epidermal growth factor receptor 2; *PIK3CA*: phosphatidylinositol-4, 5-bisphosphate 3-kinase catalytic subunit α ; *ARID1A*: AT-rich Interactive Domain-containing protein 1A; RIPA: radio-immunoprecipitation assay; PMSF: phenyl methyl sulfonyl fluoride; SDS: sodium dodecylsulfate; PAGE: polyacrylamide gel electrophoresis; PVDF:

polyvinylidene fluoride; HRP: horseradish peroxidase; CAT: carboplatin and taxane; i.p.: intraperitoneal.

Supplementary Material

Supplementary figure and tables.

<http://www.jcancer.org/v09p3196s1.pdf>

Acknowledgements

We acknowledge support to Soricimed Biopharma Inc. from the National Research Council of Canada's Industrial Research Assistance Program (project 705157), and the Atlantic Canada Opportunity Agency's Atlantic Innovation Foundation (contract number 195243) for funding various aspects of this work.

Ethics approval

The animal work was approved by the Animal Care Committee of the University of British Columbia (Application A10-0082) and followed the guidelines of the Canadian Council on Animal Care.

Availability of data and material

The datasets used and analyzed during the current study are available from the corresponding author on reasonable request.

Authors' contributions

YW: Planning and director of xenograft lab; HX: planning and execution of laboratory work with xenograft experiments; TJM: consultation and editing manuscript; TL: qPCR work and data analysis; CR: project planning, PCR validation, editing manuscript; MD: Immunohistochemistry and editing; DD: planning and manuscript revision/editing; TTI: Project management and manuscript review/revision; JMS: Project planning, data analysis, writing document, corresponding author.

Competing Interests

John M. Stewart holds shares in Soricimed Biopharma Inc. The other authors declare no potential competing interests.

References

1. Minke B. *Drosophila* mutant with a transducer defect. *Biophys Struct Mech*. 1977; 3: 59-64.
2. Montell C, Rubin GM. Molecular characterization of the *Drosophila* trp locus: a putative integral membrane protein required for phototransduction. *Neuron*. 1989; 2: 1313-23.
3. Hoenderop JG, van der Kemp AW, Hartog A, van de Graaf SF, van Os CH, Willems PH, et al. Molecular identification of the apical Ca²⁺ channel in 1, 25-dihydroxyvitamin D₃-responsive epithelia. *J Biol Chem*. 1999; 274: 8375-8.
4. Peng JB, Chen XZ, Berger UV, Vassilev PM, Tsukaguchi H, Brown EM, et al. Molecular cloning and characterization of a channel-like transporter mediating intestinal calcium absorption. *J Biol Chem*. 1999; 274: 22739-46.
5. Caterina MJ, Schumacher MA, Tominaga M, Rosen TA, Levine JD, Julius D. The capsaicin receptor: a heat-activated ion channel in the pain pathway. *Nature*. 1997; 389: 816-24.

6. Pedersen SF, Owsianik G, Nilius B. TRP channels: an overview. *Cell Calcium*. 2005; 38: 233-52.
7. Venkatachalam K, Montell C. TRP channels. *Annu Rev Biochem*. 2007; 76: 387-417.
8. Gees M, Colsoul B, Nilius B. The role of transient receptor potential cation channels in Ca²⁺ signaling. *Cold Spring Harb Perspect Biol*. 2010; 2: a003962.
9. Wu LJ, Sweet TB, Clapham DE. International Union of Basic and Clinical Pharmacology. LXXVI. Current progress in the mammalian TRP ion channel family. *Pharmacol Rev*. 2010; 62: 381-404.
10. Vennekens R, Hoenderop JG, Prenen J, Stuijver M, Willems PH, Droogmans G, et al. Permeation and gating properties of the novel epithelial Ca(2+) channel. *J Biol Chem*. 2000; 275: 3963-9.
11. Nijenhuis T, Hoenderop JG, Nilius B, Bindels RJ. (Patho)physiological implications of the novel epithelial Ca²⁺ channels TRPV5 and TRPV6. *Pflugers Arch*. 2003; 446: 401-9.
12. Peng JB, Zhuang L, Berger UV, Adam RM, Williams BJ, Brown EM, et al. CaT1 expression correlates with tumor grade in prostate cancer. *Biochem Biophys Res Commun*. 2001; 282: 729-34.
13. Bianco SD, Peng JB, Takanaga H, Suzuki Y, Crescenzi A, Kos CH, et al. Marked disturbance of calcium homeostasis in mice with targeted disruption of the Trpv6 calcium channel gene. *J Bone Miner Res*. 2007; 22: 274-85.
14. Peng JB, Chen XZ, Berger UV, Weremowicz S, Morton CC, Vassilev PM, et al. Human calcium transport protein CaT1. *Biochem Biophys Res Commun*. 2000; 278: 326-32.
15. Boddling M, Wissenbach U, Flockerzi V. The recombinant human TRPV6 channel functions as Ca²⁺ sensor in human embryonic kidney and rat basophilic leukemia cells. *J Biol Chem*. 2002; 277: 36656-64.
16. Semenova SB, Vassilieva IO, Fomina AF, Runov AL, Negulyaev YA. Endogenous expression of TRPV5 and TRPV6 calcium channels in human leukemia K562 cells. *Am J Physiol Cell Physiol*. 2009; 296: C1098-104.
17. Zhuang L, Peng JB, Tou L, Takanaga H, Adam RM, Hediger MA, et al. Calcium-selective ion channel, CaT1, is apically localized in gastrointestinal tract epithelia and is aberrantly expressed in human malignancies. *Lab Invest*. 2002; 82: 1755-64.
18. Fixemer T, Wissenbach U, Flockerzi V, Bonkhoff H. Expression of the Ca²⁺-selective cation channel TRPV6 in human prostate cancer: a novel prognostic marker for tumor progression. *Oncogene*. 2003; 22: 7858-61.
19. Wissenbach U, Niemeyer BA, Fixemer T, Schneidewind A, Trost C, Cavalie A, et al. Expression of CaT-like, a novel calcium-selective channel, correlates with the malignancy of prostate cancer. *J Biol Chem*. 2001; 276: 19461-8.
20. Wissenbach U, Niemeyer B, Himmerkus N, Fixemer T, Bonkhoff H, Flockerzi V. TRPV6 and prostate cancer: cancer growth beyond the prostate correlates with increased TRPV6 Ca²⁺ channel expression. *Biochem Biophys Res Commun*. 2004; 322: 1359-63.
21. Bolanz KA, Hediger MA, Landowski CP. The role of TRPV6 in breast carcinogenesis. *Mol Cancer Ther*. 2008; 7: 271-9.
22. Dhennin-Duthille I, Gautier M, Faouzi M, Guilbert A, Brevet M, Vaudry D, et al. High expression of transient receptor potential channels in human breast cancer epithelial cells and tissues: correlation with pathological parameters. *Cell Physiol Biochem*. 2011; 28: 813-22.
23. Peters AA, Simpson PT, Bassett JJ, Lee JM, Da Silva L, Reid LE, et al. Calcium channel TRPV6 as a potential therapeutic target in estrogen receptor-negative breast cancer. *Mol Cancer Ther*. 2012; 11: 2158-68.
24. Boddling M. TRP proteins and cancer. *Cell Signal*. 2007; 19: 617-24.
25. Prevarskaya N, Zhang L, Barritt G. TRP channels in cancer. *Biochim Biophys Acta*. 2007; 1772: 937-46.
26. Santoni G, Farfariello V, Amantini C. TRPV channels in tumor growth and progression. *Adv Exp Med Biol*. 2011; 704: 947-67.
27. Lehen'kyi V, Raphael M, Prevarskaya N. The role of the TRPV6 channel in cancer. *J Physiol*. 2012; 590: 1369-76.
28. Ouadid-Ahidouch H, Dhennin-Duthille I, Gautier M, Sevestre H, Ahidouch A. TRP channels: diagnostic markers and therapeutic targets for breast cancer? *Trends Mol Med*. 2013; 19: 117-24.
29. Huber SM. Oncochannels. *Cell Calcium*. 2013; 53: 241-55.
30. Schwarz EC, Wissenbach U, Niemeyer BA, Strauss B, Philipp SE, Flockerzi V, et al. TRPV6 potentiates calcium-dependent cell proliferation. *Cell Calcium*. 2006; 39: 163-73.
31. Crabtree GR, Olson EN. NFAT signaling: choreographing the social lives of cells. *Cell*. 2002; 109 Suppl: S67-79.
32. Masuda ES, Imamura R, Amasaki Y, Arai K, Arai N. Signalling into the T-cell nucleus: NFAT regulation. *Cell Signal*. 1998; 10: 599-611.
33. Saygili E, Rana OR, Meyer C, Gemein C, Andrzejewski MG, Ludwig A, et al. The angiotensin-calcineurin-NFAT pathway mediates stretch-induced up-regulation of matrix metalloproteinases-2/-9 in atrial myocytes. *Basic Res Cardiol*. 2009; 104: 435-48.
34. Liu S, Umez-Goto M, Murph M, Lu Y, Liu W, Zhang F, et al. Expression of autotaxin and lysophosphatidic acid receptors increases mammary tumorigenesis, invasion, and metastases. *Cancer Cell*. 2009; 15: 539-50.
35. Mancini M, Toker A. NFAT proteins: emerging roles in cancer progression. *Nat Rev Cancer*. 2009; 9: 810-20.
36. Gomez J, Martinez AC, Gonzalez A, Garcia A, Rebollo A. The Bcl-2 gene is differentially regulated by IL-2 and IL-4: role of the transcription factor NF-AT. *Oncogene*. 1998; 17: 1235-43.

37. Lehen'kyi V, Flourakis M, Skryma R, Prevarskaya N. TRPV6 channel controls prostate cancer cell proliferation via Ca(2+)/NFAT-dependent pathways. *Oncogene*. 2007; 26: 7380-5.
38. Quang CT, Leboucher S, Passaro D, Fuhrmann L, Nourieh M, Vincent-Salomon A, et al. The calcineurin/NFAT pathway is activated in diagnostic breast cancer cases and is essential to survival and metastasis of mammary cancer cells. *Cell Death Dis*. 2015; 6: e1658.
39. Raphael M, Lehen'kyi V, Vandenberghe M, Beck B, Khalimonchik S, Vanden Abeele F, et al. TRPV6 calcium channel translocates to the plasma membrane via Orai1-mediated mechanism and controls cancer cell survival. *Proc Natl Acad Sci U S A*. 2014; 111: E3870-9.
40. Skrzypski M, Khajavi N, Mergler S, Szczepankiewicz D, Kolodziejski PA, Metzke D, et al. TRPV6 channel modulates proliferation of insulin secreting INS-1E beta cell line. *Biochim Biophys Acta*. 2015; 1853: 3202-10.
41. Song H, Dong M, Zhou J, Sheng W, Li X, Gao W. Expression and prognostic significance of TRPV6 in the development and progression of pancreatic cancer. *Oncol Rep*. 2018.
42. Bowen CV, DeBay D, Ewart HS, Gallant P, Gormley S, Ilenchuk TT, et al. In vivo detection of human TRPV6-rich tumors with anti-cancer peptides derived from soricidin. *PLoS One*. 2013; 8: e58866.
43. Kobel M, Kalloger SE, Boyd N, McKinney S, Mehl E, Palmer C, et al. Ovarian carcinoma subtypes are different diseases: implications for biomarker studies. *PLoS Med*. 2008; 5: e232.
44. Fu S, Hirte H, Welch S, Ilenchuk TT, Lutes T, Rice C, et al. First-in-human phase I study of SOR-C13, a TRPV6 calcium channel inhibitor, in patients with advanced solid tumors. *Invest New Drugs*. 2017.
45. Domcke S, Sinha R, Levine DA, Sander C, Schultz N. Evaluating cell lines as tumour models by comparison of genomic profiles. *Nat Commun*. 2013; 4: 2126.
46. Wiegand KC, Shah SP, Al-Agha OM, Zhao Y, Tse K, Zeng T, et al. ARID1A mutations in endometriosis-associated ovarian carcinomas. *N Engl J Med*. 2010; 363: 1532-43.
47. Shaw TJ, Senterman MK, Dawson K, Crane CA, Vanderhyden BC. Characterization of intraperitoneal, orthotopic, and metastatic xenograft models of human ovarian cancer. *Mol Ther*. 2004; 10: 1032-42.
48. Hirnet D, Olausson J, Fecher-Trost C, Boddling M, Nastainczyk W, Wissenbach U, et al. The TRPV6 gene, cDNA and protein. *Cell Calcium*. 2003; 33: 509-18.
49. Lu P, Boros S, Chang Q, Bindels RJ, Hoenderop JG. The beta-glucuronidase klotho exclusively activates the epithelial Ca2+ channels TRPV5 and TRPV6. *Nephrol Dial Transplant*. 2008; 23: 3397-402.
50. Lu L, Katsaros D, Wiley A, de la Longrais IA, Puopolo M, Yu H. Klotho expression in epithelial ovarian cancer and its association with insulin-like growth factors and disease progression. *Cancer Invest*. 2008; 26: 185-92.
51. Cha SK, Ortega B, Kurosu H, Rosenblatt KP, Kuro OM, Huang CL. Removal of sialic acid involving Klotho causes cell-surface retention of TRPV5 channel via binding to galectin-1. *Proc Natl Acad Sci U S A*. 2008; 105: 9805-10.
52. Chang Q, Hoefs S, van der Kemp AW, Topala CN, Bindels RJ, Hoenderop JG. The beta-glucuronidase klotho hydrolyzes and activates the TRPV5 channel. *Science*. 2005; 310: 490-3.